Otolith stimulation induces *c-Fos* expression in vestibular and precerebellar nuclei in cats and squirrel monkeys

Joan S. Baizer[*] and **Will L. Corwin**
Department of Physiology and Biophysics, University at Buffalo, School of Medicine and Biomedical Sciences, 123 Sherman Hall, Buffalo, NY 14214, 716-829-3096, baizer@buffalo.edu

James F. Baker
Department of Physiology, Physiology/Medical, Ward 5-071, M211, Northwestern University Medical School, 303 East Chicago Avenue, Chicago, ILL 60611-3008, 312-503-1322, j-baker@northwestern.edu

Abstract

Vestibular information is critical for the control of balance, posture, and eye movements. Signals from the receptors, the semicircular canals and otoliths, are carried by the eighth nerve and distributed to the four nuclei of the vestibular nuclear complex, the VNC. However, anatomical and physiological data suggest that many additional brainstem nuclei are engaged in the processing of vestibular signals and generation of motor responses. In order to assess the role of these structures in vestibular functions, we have used expression of the immediate early gene *c-Fos* as a marker for neurons activated by stimulation of the otoliths or the semicircular canals. Excitation of the otolith organs resulted in widespread *c-Fos* expression in the VNC, but also in other nuclei, including the external cuneate nucleus, the postpyramidal nucleus of the raphé, the nucleus prepositus hypoglossi, the subtrigeminal nucleus, the pontine nuclei, the dorsal tegmental nucleus, the locus coeruleus and the reticular formation. Rotations that excited the semicircular canals were much less effective in inducing *c-Fos* expression. The large number of brainstem nuclei that showed *c-Fos* expression may reflect the multiple functions of the vestibular system. Some of these neurons may be involved in sensory processing of the vestibular signals, while others provide input to the vestibulo-ocular, vestibulocollic and vestibulospinal reflexes, or mediate changes in autonomic function. The data show that otolith stimulation engages brainstem structures both within and outside of the VNC, many of which project to the cerebellum.

INTRODUCTION

Signals from the vestibular receptors, the semicircular canals and otolith organs, are essential for the control of balance, posture and eye movements. Vestibular information is carried by the eighth cranial nerve and distributed to the four nuclei that comprise the vestibular nuclear complex (VNC), and to the cerebellum (Barmack, 2003; Büttner-Ennever and Gerrits, 2004; Carleton and Carpenter, 1984; Gerrits, 1990; Korte, 1979; Korte and Mugnaini, 1979). The connections and response properties of the nuclei of the VNC have been extensively studied in many species (reviews in Barmack, 2003; Büttner-Ennever and

Gerrits, 2004; Büttner-Ennever, 1992). The vestibular nerve projects to nuclei outside of the VNC, for example the external cuneate nucleus (ECu), the subtrigeminal nucleus (Sub; Carleton and Carpenter, 1984; Korte, 1979) and possibly both the nucleus prepositus (PrH) and the paravestibular nucleus (PaVe; Kevetter et al., 2004). In addition, there are projections from the VNC to other brainstem nuclei, for example PrH, the nucleus of the seventh cranial nerve, and reticular and pontine cell groups (Belknap and McCrea, 1988; Gerrits et al., 1985a; Ladpli and Brodal, 1968; Shaw and Baker, 1983).

We wished to determine which of these structures were activated by different vestibular inputs. One way to assess neuronal activation is to look for the expression of the immediate early gene *c-Fos* (Morgan and Curran, 1991). *c-Fos* expression has been widely demonstrated in the vestibular brainstem in response to deafferentation (vestibular compensation; references in Cirelli et al., 1996; D'Ascanio et al., 1998; Darlington et al., 1996; Darlington and Smith, 1996; Duflo et al., 1999; Jensen, 1979; Kaufman et al., 1993; Kaufman et al., 1999; Kitahara et al., 1995; Kitahara et al., 1997; Vibert et al., 1999) and vestibular stimulation, both in the laboratory and also in the microgravity conditions of space flight (Kaufman et al., 1992; Kaufman et al., 1993; Kaufman, 1996; Kaufman et al., 1999; Kaufman et al., 2003; Lai et al., 2004; Marshburn et al., 1997; Saxon et al., 2001; Shinder et al., 2005a; Shinder et al., 2005b). Most of the studies of *c-Fos* expression in vestibular compensation, and all of the studies using vestibular stimulation, have been done in rodents. The cat and the squirrel monkey have been used extensively in studies of vestibular physiology and anatomy. Here we have used otolith organ and semicircular canal stimulation paradigms and examined *c-Fos* expression in the medulla and pons of these animals. We wished to do an initial comparison of the effectiveness of otolith and semicircular canal stimulation in causing *c-Fos* expression. Accordingly, we used earth-horizontal axis, continuous rotation stimuli at a constant velocity, because constant rotation about non-vertical axes provides strong, modulated excitation of the vestibular otoliths (Angelaki and Hess, 1995; Pettorossi et al., 2001; Raphan and Schnabolk, 1988) with only brief, initial stimulation of the semicircular canals (time constant ~5 s. (Blanks et al., 1975; Goldberg and Fernandez, 1971). These stimuli allowed us to test otolith-mediated *c-Fos* expression independently from canal-mediated *c-Fos* expression.

The pattern of *c-Fos* expression in the vestibulocerebellum in these animals has been reported (Sekerkova et al., 2005); some of the results for the brainstem have been reported in an abstract (Baker and Baizer, 2000). Brains from these animals have also been used in anatomical experiments on the neurochemical organization of the vestibular brainstem (Baizer and Baker, 2005a; Baizer and Baker, 2005b; Baizer and Baker, 2006a; Baizer and Baker, 2006b; Baizer, 2009).

RESULTS

CATS

We analyzed sections through the entire extent of the VNC, as well as more anterior sections through the level of the pontine nuclei (Pn). The number and distribution of Fos-immunoreactive nuclei in the brainstem varied with stimulation paradigm. The otolith stimulation paradigms resulted in greater *c-Fos* expression than did the semicircular canal stimulation paradigms. All cats (CAT2, 3, 4, 6, 7, and 9) that were subjected to stimulation of the otolith organs in conditions that engaged vestibulo-oculomotor reflexes (Methods, conditions 1-4) had widespread c-*Fos* expression. Fewer labeled cells in the same structures were seen in cats that were subjected to stimulation of the semicircular canals (conditions 5 and 6; CAT8, 10).

OTOLITH STIMULATION

Figure 1A is a photomontage illustrating the distribution of labeled cells on a section at about P10.0 in CAT2; this animal experienced continuous rotation of the otolith organs in the test session. Figure 1B shows a plot of this same section. The inset identifies the outlined nuclei at this stereotaxic level. Comparison of the two panels illustrates our criterion for labeled cells. In the VNC, there are many labeled nuclei in both the medial (MVe) and inferior (SpVe) vestibular nuclei (Fig. 1A, B). The distribution on the two sides of the brain is similar. Cells with labeled nuclei are distributed throughout SpVe but are denser dorsally than ventrally in the MVe. There are also labeled cells in the nucleus prepositus hypoglossi (PrH). Outside the VNC, there was a high density of labeled cells in the subtrigeminal nucleus (Sub), a small roughly triangular nucleus just ventral to the spinal trigeminal tract (5ST). Labeled cells are scattered throughout the external cuneate nucleus (ECu); there are many labeled cells in the postpyramidal nucleus of the raphé (RPa; PPR in the Berman atlas), and labeled cells are scattered throughout the reticular formation (RF). There is only an occasional cell labeled in any subdivision of the inferior olive (IO). There are labeled cells throughout the anterior-posterior extent of each structure in which labeled cells are present at P10.

Figure 2A shows the distribution of labeled cells from the same case on a section about 1.5 mm anterior to the one shown in Fig. 1. Labeled cells are again seen in PrH, MVe, SpVe, Sub, RPA, RF and ECu. In addition, there are labeled cells in the facial nucleus (7). There are almost no labeled nuclei in the lateral vestibular nucleus (LVe). At a more anterior level, there are labeled cells in the superior vestibular nucleus (SuVe; Fig. 2B). At about P4.0, a level anterior to PrH and the VNC, there are many labeled cells in the dorsal tegmental nucleus (DT; Fig. 2D). At about P1.5 there is a very high density of labeled cells in the pontine nuclei (Pn), in all divisions (Fig. 2C). This general distribution of labeled cells was seen in all five other cats (CAT3, 4, 6, 7, 9) experiencing otolith stimulation during the test session. Figure 3 shows the distribution of cells on sections at about the same A-P level as in Figure 1 from CAT4 and CAT7, which had identical stimulation parameters, and CAT3 for which the stimulus duration was longer (180 min) and the speed was higher ($100°$ s^{-1}). In all three animals, there are labeled cells in the same structures as in CAT2. The lower Fos-immunoreactivity in CAT3 may reflect the limited time course of *c-Fos* gene expression (Hughes and Dragunow, 1995), rather than a lower effectiveness of the high velocity of rotation; a recent study found a reduction in Fos-immunoreactivity in somatosensory cortex beyond two hours, despite the persistently painful stimulation of bee venom (Chang et al., 2008).

There were two additional otolith stimulation paradigms that also resulted in labeled cells in the same set of nuclei. CAT6 was subjected to sinusoidal oscillation of otoliths, and CAT9 was subjected to constant velocity rotation about an earth-horizontal roll axis (Fig. 4). Thus, Fos-immunoreactive cells were found in the same set of brainstem structures for all otolith stimulation paradigms. The label in CAT6 shows that rotation need not be the constant velocity stimulus chosen for the first three stimulation paradigms; oscillatory stimulation results in similar Fos-immunoreactivity. The label in CAT9 confirms that stimulation of horizontal oculomotor systems, present under all the other stimulus conditions, is not a requirement for Fos-immunoreactivity.

SEMICIRCULAR CANAL STIMULATION

In the two animals, CAT8 and CAT10, that experienced semicircular canal stimulation alone, labeled cells were found in the same set of structures, but there were many fewer of them than in the otolith stimulation cases (Fig. 5). Table 1 summarizes the numbers of labeled cells found in the different cats.

SQUIRREL MONKEYS

In the squirrel monkey, labeled cells in the VNC and throughout the brainstem were also seen following otolith stimulation. The three dimensional layout of the VNC is different in cats and squirrel monkeys, so that different sets of structures are seen on single coronal sections in the two species. Figure 6A shows the distribution of cells on a plot of a section from SM5 at about P3.5. At this level, labeled cells are present in the SpVe, MVe, PrH and the RF. In contrast to the cat (Fig. 2A), there are very few labeled nuclei in the DCN. More anteriorly, there were virtually no labeled cells in the LVe and only a scattering in the SuVe. At still more anterior levels, there were many labeled cells in the ventral raphé, in the DT and in the Pn (not shown). The highest density of labeled cells in any brainstem structure is in the mesencephalic nucleus of the trigeminal (Me5, Fig. 6B). The distribution of cells in the other two animals subjected to this paradigm is similar, but the density was not as great. In the squirrel monkey subjected to vertical axis rotation during the test session (condition 5, see Methods) there were very few labeled cells anywhere in the brainstem.

DISCUSSION

In response to otolith stimulation we found expression of the Fos protein in many neurons in multiple brainstem structures. Some labeled neurons may be involved in sensory analysis, while others may be more directly involved in mediating reflex responses either directly or via cerebellar relays. We will consider the structures in which we saw labeled cells with respect to their potential roles in vestibulo-motor circuitry. We will also compare the distribution of labeled cells that we see with that reported in other studies using vestibular stimulation or vestibular deafferentation.

VNC, PrH

Labeled cells were seen in three of the four nuclei of the VNC and in PrH. Vestibular stimulation provides input to the vestibulooocular, vestibulocollic and vestibulospinal reflexes (references in Gerrits, 1990), as well as affecting cardiovascular control and blood pressure (Jian et al., 1999; Yates et al., 2000). Labeled cells are found throughout the region of the VNC from which projections to the oculomotor cranial nerve nuclei arise (Gacek, 1977; Graybiel and Hartwieg, 1974; Hoddevik et al., 1991; Spencer et al., 1989), consistent with a role in the control of the vestibuloocular reflex. PrH projects to the cranial nerve nuclei and to the cerebellum (Belknap and McCrea, 1988; McCrea et al., 1979; McCrea and Baker, 1985). PrH could have a role in processing the storage (Raphan et al., 1979) and estimation of head velocity (Raphan and Cohen, 1988; discussion and references in Sekerkova et al. 2005). It also has a role in the oculomotor integration that generates a gaze-holding orbital position signal (Cannon and Robinson, 1987; Fukushima and Kaneko, 1995; Sylvestre et al., 2003).

Sub, ECu, Pn

We saw labeled cells in two cerebellar relay nuclei, the Sub and the ECu. While not included in the VNC, the ECu receives direct input from the vestibular nerve (Carleton and Carpenter, 1984; Korte, 1979) and projects to the cerebellum (Gerrits et al., 1985b; Somana and Walberg, 1980). The Sub may also receive direct input from the vestibular nerve, although such a projection is not consistently found (Carleton and Carpenter, 1984; Korte, 1979). The Sub projects to the same region of the cerebellum as the vestibular nuclei and PrH (Sato et al., 1989). There are also anatomical data that suggest that the caudal Sub may be important for the control of respiration (Lois et al., 2009; Panneton et al., 2000).

There was a very high density of labeled nuclei in another cerebellar relay, the pontine gray. Pontine cells may receive vestibular information either directly from the vestibular nerve (Gerrits et al., 1985a) or indirectly via the vestibular cortex.

Otolith vs. semicircular canal stimulation

There were many fewer labeled cells in the animals that were subjected to stimulation of only the semicircular canals (CAT8, 10). This might reflect the lack of engagement of the "velocity estimation" central circuitry that underlies continuous nystagmus (Raphan and Cohen, 1988) and the absence of the prolonged vestibular nystagmus that occurred in the animals subjected to continuous rotation in yaw or roll. The acclimatization sessions were intended to minimize general factors such as autonomic effects or anxiety (Balaban, 2002), but another stimulus for Fos expression could have been the repeating pattern of vestibular-autonomic activation by those continuous rotations. For example, blood pressure regulation mechanisms were modulated at the rate of rotation by the changing gravitational position of the head and body (Kerman and Yates, 1998). In the acclimatization sessions this modulation was much more gradual, determined by the ~1°/s offset velocity. There are projections from a utonomic nuclei to vestibular nuclei (Balaban and Beryozkin, 1994; Balaban and Porter, 1998) that could have been responsible for Fos expression, and projections from vestibular nuclei to autonomic centers (Balaban, 2004) that could have resulted in Fos expression in other brainstem areas.

Comparison with other studies

The MVe, SpVe, and SuVe and PrH are the nuclei in which *c-Fos* expression is reported after various vestibular stimulation paradigms and with short or long-term lesions of the vestibular nerve or labyrinth (Kaufman et al., 1992; Kaufman et al., 1999; Shinder et al., 2005b). The scarcity of labeled cells in the LVe that we see is in agreement with several studies in rodents, and one study in the cat (Duflo et al., 1999). That study suggested that the scarcity of Fos-positive cells in the LVe was related to the reduction in LVe neuron activity following labyrinthectomy. However, our stimulation paradigms almost surely increased LVe neuron activity. Cells in this nucleus may express other transcription factors in response to activity. Different transcription factors may be expressed in different structures or in the same structure in different conditions. For example, cells in the facial nerve nucleus express *c-Jun* but not *c-Fos* in response to axotomy (Haas et al., 1993; Moran and Graeber, 2004), but express *c-Fos* in our paradigm (Fig. 2A).

Fos expression in the pontine nuclei was also seen in rats exposed to low gravity conditions (d'Ascanio et al., 2003), and in cats after section of the vestibular nerve (Duflo et al., 1999). Marshburn et al. (1997) found cells in the dorsomedial and dorsolateral tegmental nuclei of the gerbil after hypergravity stimulation, and cells were seen in these nuclei in the cat after neurectomy (Duflo et al., 1999). Studies in rodents report labeled cells in LC both from stimulation (Kaufman et al., 1992; Lai et al., 2004; Marshburn et al., 1997) and lesion paradigms (D'Ascanio et al., 1998). Labeled cells in this region were seen after vestibular neurectomy in the cat (Duflo et al., 1999).

We saw very few labeled cells in the IO. *c-Fos* expression is seen in the IO of rodents with vestibular stimulation (Chen et al., 2003; Kaufman et al., 1992; Marshburn et al., 1997; Shinder et al., 2005b), as well as during vestibular compensation (Cirelli et al., 1996; Duflo et al., 1999; Kaufman, 2005; Kitahara et al., 1995). These data raise the possibility of species differences in the vestibular role of the olivocerebellar system.

Our label patterns were all bilaterally symmetrical. Asymmetry in changes in gene expression is reported after temporary or permanent unilateral deafferentation (Duflo et al.,

1999; Kaufman et al., 1993; Kaufman, 2005; Saxon, 2003; Shinder et al., 2006). However, bilateral symmetry in the numbers of Fos-immunoreactive neurons has been reported in intact animals (Kaufman et al., 1992; Kaufman, 2005; Lai et al., 2004).

Significance of *c-Fos* expression

c-Fos expression is sometimes interpreted as a marker for activity (Alger et al., 2009; for examples see Guo et al., 2005; Muigg et al., 2009; Snyder et al., 2009). In other studies, for example studies of vestibular compensation and studies of the effects of addictive drugs, the emphasis is on changes in cell structure or function that occur as a consequence of the experimental treatment, with expression of the *c-Fos* gene a first step (reviews in Kaufman, 2005; Nestler, 2008). We are using expression of the Fos protein as an indicator of activity but the *c-Fos* expression we see may well be a marker for plasticity elicited by our stimulus paradigms. The vestibular paradigms we used provided activation outside the normal physiological range, with the potential for inducing plastic changes in both sensory and motor components of the circuitry. What might those plastic changes be? Since cells immunoreactive to the Fos protein were found in multiple structures with different connections and functions it is likely that there is a diversity of subsequent neuronal changes that vary as a function of the neurochemistry of the different cells.

In summary these experiments have shown that vestibular input activates, and has the potential for driving plastic changes in, a large set of brainstem nuclei that extends well beyond the traditionally defined four vestibular nuclei. Some, but not all, of these nuclei have well-established roles in vestibular function. The roles of the subtrigeminal and external cuneate nuclei have yet to be defined.

EXPERIMENTAL PROCEDURE

Animals and surgical procedures

We used eight domestic cats and four squirrel monkeys. The animals were purchased from commercial breeders and housed in the animal care facility of Northwestern University. All experiments followed the principles of laboratory animal care set forth by the National Institutes of Health in the Guide for Care and Use of Laboratory Animals, and were approved by the Institutional Animal Care and Use Committee of Northwestern University. Animals were fitted with a head restraint fixture under isoflurane anesthesia using sterile surgical procedures. Animals were intubated after a restraining dose of Ketamine (20 mg/kg, i.m.), and then maintained on isoflurane (1-1.5%) in oxygen. EKG, respiration, blood oxygen saturation, and end tidal CO_2 were monitored. Eight evenly spaced holes (1.05 mm diam.) were tapped across the dorsal surface of the skull. Small stainless steel screws (0-80) were carefully threaded through these holes without puncturing the dura mater. The screws and dental acrylic were used to secure a rectangular metal fixture aligned with the stereotaxic planes, so that the head could be fixed in our rotation apparatus at a known stereotaxic posture. Animals were allowed at least a week to recover from surgery before they were brought to the laboratory for behavioral acclimatization and test sessions.

Behavioral sessions

The experimental conditions have been described previously (Sekerkova et al., 2005). Animals were securely restrained in a servomotor powered vestibular rotation apparatus, with the head fixed either in the stereotaxic plane (squirrel monkeys, Killian and Baker, 2005), or at a 27° downward pitch from t he stereotaxic position (cats, Baker and Peterson, 1991), the downward pitch chosen to minimize vertical canal stimulation by yaw rotation (Curthoys et al., 1977). In every stimulus condition the axis of rotation was centered on the C1-C2 neck joint, approximately the axis of voluntary head rotation of cats. All but one of

the animals were subjected to five or more days of 90 min *"acclimatization sessions"* in order to minimize brainstem *c-Fos* expression in response to novelty or stress (Melia et al., 1994; O'Hara et al., 1993), and to allow adaptation to the novel somatosensory stimulation. The same vestibular stimulus waveform was used for each day of acclimatization. The stimulus axis was always oriented to be the same as for the test run. For all but one animal, yaw axis rotations about the animal's dorso-ventral axis were used, in order to activate horizontal vestibular reflexes. In one cat, roll rotations about the animal's rostro-caudal axis were used, to activate vertical vestibular reflexes. All sessions were held in complete darkness with the only additional stimulation being noises made by the experimenters to encourage alertness of the animals. The stimulus waveform during acclimatization sessions was a 0.2 Hz, 30° amplitude sinusoid (38° s^{-1} peak velocity) with an added constant offset velocity of about 1° per second (s^{-1}) that resulted in a gradual progression through all positions around the rotation axis. This stimulus provided semicircular canal activation and exposed the animal to all the body orientations encountered during the test session. The low offset velocity did not produce a measurable bias velocity of vestibular nystagmus. On the sixth day, the animal was subjected to a test session, which was either one of four procedures (1-4) for otolith organ stimulation, three of which encouraged prolonged vestibular nystagmus (1-3), or one of two procedures (5, 6) that instead stimulated semicircular canals and not the otolith organs.

Otolith Stimulation Paradigms

1. Continuous rotation, yaw, 90 min (CAT2, 4, 7; SM2, 3, 5)—In each session, the animal was subjected to 90 min. of rotation about an earth-horizontal yaw axis. Acclimatization sessions were 0.2 Hz, 30° amplitude rotations with a 1° s^{-1} offset velocity. The test session was 90 min of 60° s^{-1} constant offset velocity rotation about an earth-horizontal yaw axis, rotation to the animal's left. The test session provided a strong and prolonged stimulus to the otolith organs and elicited the continuous horizontal vestibular nystagmus characteristic of head angular velocity estimation (Raphan and Schnabolk, 1988).

2. Continuous rotation, yaw, 180 min (CAT3)—Acclimatization sessions were 90 min of 0.2 Hz, 30° amplitude rotations with a 1° s^{-1} offset velocity. The test session was 180 min of 100° s^{-1} constant velocity rotation about an earth-horizontal yaw axis, rotation to the animal's left. Thus, the test session provided a strong and very prolonged otolith stimulus for continuous horizontal vestibular nystagmus.

3. Continuous rotation, roll, 90 min (CAT9)—All rotations were about an earth-horizontal roll axis for 90 min. Acclimatization sessions were 0.2 Hz, 30° amplitude, 1° s^{-1} offset velocity rotations. The test session was 90 min of 60°s^{-1} constant velocity rotation about an earth-horizontal roll axis, rotation to the animal's left (left ear down rotation). The test session provided a strong and prolonged otolith stimulus for continuous torsional vestibular nystagmus.

4. Sinusoidal oscillation of otoliths, yaw, 90 min (CAT6)—All rotations were about a horizontal yaw axis for 90 min. Acclimatization sessions were 0.2 Hz, 30° amplitude, 1° s^{-1} offset velocity rotations about an earth-horizontal yaw axis. The test session was the same as the acclimatization sessions. There was the same gradually shifting pattern of otolith stimulation during acclimatization and test sessions, without a strong stimulus for continuous vestibular nystagmus.

Semicircular Canal Stimulation Paradigms

5. Sinusoidal oscillation of canals, yaw, 90 min (CAT8, SM4)—All rotations were about a vertical yaw axis for 90 min. Acclimatization sessions were 0.2 Hz 30° amplitude,

$1°$ s $^{-1}$ offset velocity rotations about an earth-vertical yaw axis. The test session was the same as the acclimatization sessions, with no significant otolith stimulation during either acclimatization or test sessions. These animals provided a control for comparison to the animals subjected to otolith stimulation and more intense canal stimulation.

6. Rapid sinusoidal oscillation of canals, yaw, 90 min (CAT10)—All rotations were about a vertical yaw axis for 90 min. Acclimatization sessions were 0.2 Hz, $30°$ amplitude, $1°$ s $^{-1}$ offset velocity rotations about an earth-vertical yaw axis. The test session was 90 min of 0.2 Hz rotations about an earth-vertical yaw axis, $180°$ amplitude ($226°$ s $^{-1}$ peak velocity), providing strong stimulation to the horizontal canals, without an otolith stimulus for continuous vestibular nystagmus.

Tissue preparation—At the end of the experimental vestibular stimulation, animals were deeply anesthetized with intravenous Sodium Pentobarbital (40 mg/kg i.v.), as quickly as possible, and then perfused through the aorta with 0.9% saline followed by 4% paraformaldehyde in phosphate-buffered saline (PBS).The brains were removed and the brainstem was dissected from the rest of the brain at a level between the pons and midbrain. The anterior limit of the dissection, and the amount of the midbrain available for study varied among the cases. The cerebellum was dissected free in all animals for use in other experiments (Sekerkova et al., 2005), causing some damage to the superior vestibular nucleus. The brainstems were then cryoprotected in graded concentrations of sucrose in PBS (10%, 20% and 30%), quick frozen in $-70°$ C isopentane or in a cryoprotectant solution (30% ethylene glycol and 30% glycerol in phosphate buffer, PB). The tissue blocks were covered with that solution and stored in a $-70°$ C freezer until cutting. The brainstem of one case was embedded in an albumin-gelatin matrix. Frozen frontal sections 33 μm (squirrel monkey) or 40-50 μm (cat) of the brainstems were cut on an American Optical sliding microtome. All sections were collected and stored at $-20°$ C in tissue culture wells in the cryoprotectant solution.

Immunohistochemistry—Sections were processed for immunoreactivity to the Fos protein using standard immunohistochemical techniques and the Vector ABC method. Briefly, sections were removed from the cryoprotectant, rinsed in PBS (all rinses were $3\times10'$ each), and incubated in a solution of PBS with 5% nonfat dry milk, 0.3 %Triton-X100, 1.5% normal serum, and an antibody to Fos (Oncogene, Ab5, 1:5000 cats; 1:10,000 squirrel monkeys) overnight on a tissue shaker at $4°$ C. Sections were then rinsed in PBS and incubated in an anti-rabbit IgG secondary antibody (Vectakit, Vector Laboratories) in PBS with 0.3 % Triton X-100 and 1.5 % normal serum for one hour at room temperature on a shaker, rinsed again, and incubated for one hour in the Vector ABC solution (according to manufacturer instructions) on a rocker at room temperature. Immunoreactivity was visualized by incubating sections in 3,3′-diaminobenzidine (DAB, Sigma) with .0015-.003% H_2O_2 in 0.01M PBS. Staining on some sections was enhanced with the addition of nickel ammonium sulfate (NAS) and cobalt chloride, or NAS alone to the DAB solution (Adams, 1981). Control sections from each case were processed with the primary antibody omitted from the initial solution. No immunostaining was seen when the primary antibody was omitted. Sections were then mounted onto gelled glass slides, dehydrated in graded alcohol concentrations, cleared in Histosol (National Diagnostics) and coverslipped with Permount (Fisher Scientific).

Data analysis and photography—We used the Berman (1968) atlas of the cat brainstem to determine the approximate stereotaxic anterior-posterior (A-P) levels of the cat sections, and the atlas of Emmers and Akert (1963) for the squirrel monkey sections. We follow the terminology and abbreviations of Büttner-Ennever and Gerrits (2004) for the four

nuclei of the VNC and other brainstem structures, with the exception of the subtrigeminal or infratrigeminal nucleus, for which we use "Sub". We examined the sections with a Leitz Dialux 20 light microscope. Immunoreactivity for the Fos protein was seen as darkly stained round or oval nuclei. Cell nuclei varied in darkness from light brown to dark brown to almost black. We used MDplot software (Accustage, Shoreview, MN) to plot the distribution of labeled cells on outlines of sections through the brainstem at the same stereotaxic levels for each case, P10 for the cats and P3 for the squirrel monkeys. For cat2, we made an additional plot at a level between P8.5 and P9.2 (Fig. 2A). The person who did the plots was blind to the conditions of each case, and the same person did all of the plots. To make the plots, we first drew an outline of the entire section, then outlined the MVe, SpVe, PrH, Sub, RPa and ECu and finally marked all cells with darkly stained nuclei. The plots were printed with MDplot software, scanned, and the images incorporated in figures using Adobe Photoshop software. We used the MDPlot software to count the number of labeled cells in the different outlined structures. Instead of a quantitative analysis comparing the numbers of labeled cells across many animals subjected to a single paradigm, we chose to focus this study on qualitative identification of brainstem nuclei that are involved in the analysis of vestibular input and elaboration of motor responses, and so animals were subjected to several different stimulation paradigms intended to encompass a wide variety of vestibular stimuli.

For the photomicrographs, digital images were captured using a SPOT Insight Color Mosaic camera (1200 × 1600 pixels) mounted on a Leitz Dialux 20 microscope. The photomontage (Fig. 1A) was made using the "panorama" feature of a Zeiss Axioimager Z1 microscope, and Zeiss software.

Acknowledgments

REFERENCES

Adams JC. Heavy metal intensification of DAB-based HRP reaction product. J Histochem Cytochem. 1981; 29:775. [PubMed: 7252134]

Alger SJ, Maasch SN, Riters LV. Lesions to the medial preoptic nucleus affect immediate early gene immunolabeling in brain regions involved in song control and social behavior in male European starlings. Eur J Neurosci. 2009; 29:970–82. [PubMed: 19245371]

Angelaki DE, Hess BJ. Lesion of the nodulus and ventral uvula abolish steady-state off-vertical axis otolith response. J Neurophysiol. 1995; 73:1716–20. [PubMed: 7643178]

Baizer J, Baker J. Immunoreactivity for calcium-binding proteins defines subregions of the vestibular nuclear complex of the cat. Exp Brain Res. 2005a; 164:78–91. [PubMed: 15662522]

Baizer JS, Baker JF. Immunoreactivity for calcium-binding proteins defines subregions of the vestibular nuclear complex of the cat. Exp Brain Res. 2005b; 164:78–91. [PubMed: 15662522]

Baizer JS, Baker JF. Immunoreactivity for calretinin and calbindin in the vestibular nuclear complex of the monkey. Exp Brain Res. 2006a; 172:103–13. [PubMed: 16369782]

Baizer JS, Baker JF. Neurochemically defined cell columns in the nucleus prepositus hypoglossi of the cat and monkey. Brain Res. 2006b; 1094:127–37. [PubMed: 16701575]

Baizer JS. Nonphosphorylated neurofilament protein is expressed by scattered neurons in the vestibular and precerebellar brainstem. Brain Res. 2009; 1298:46–56. [PubMed: 19728992]

Baker J, Baizer J. Prolonged horizontal rotation induces c-fos expression in the vestibular nuclear complex of the cat. Neurosci Abs. 2000:28.

Baker JF, Peterson BW. Excitation of the extraocular muscles in decerebrate cats during the vestibulo-ocular reflex in three-dimensional space. Exp Brain Res. 1991; 84:266–78. [PubMed: 2065733]

Balaban CD, Beryozkin G. Vestibular nucleus projections to nucleus tractus solitarius and the dorsal motor nucleus of the vagus nerve: potential substrates for vestibulo-autonomic interactions. Exp Brain Res. 1994; 98:200–12. [PubMed: 8050507]

Balaban CD, Porter JD. Neuroanatomic substrates for vestibulo-autonomic interactions. J Vestib Res. 1998; 8:7–16. [PubMed: 9416584]

Balaban CD. Neural substrates linking balance control and anxiety. Physiol Behav. 2002; 77:469–75. [PubMed: 12526985]

Balaban CD. Projections from the parabrachial nucleus to the vestibular nuclei: potential substrates for autonomic and limbic influences on vestibular responses. Brain Res. 2004; 996:126–37. [PubMed: 14670639]

Barmack NH. Central vestibular system: vestibular nuclei and posterior cerebellum. Brain Res Bull. 2003; 60:511–41. [PubMed: 12787870]

Belknap DB, McCrea RA. Anatomical connections of the prepositus and abducens nuclei in the squirrel monkey. J Comp Neurol. 1988; 268:13–28. [PubMed: 3346381]

Berman, A. The brain stem of the cat. University of Wisconsin Press; Madison, Wisconsin: 1968.

Blanks RH, Estes MS, Markham CH. Physiologic characteristics of vestibular first-order canal neurons in the cat. II. Response to constant angular acceleration. J Neurophysiol. 1975; 38:1250–68. [PubMed: 809548]

Büttner-Ennever, J.; Gerrits, N. Vestibular System. In: Paxinos, G.; Mai, JK., editors. The Human Nervous System. Elsevier; Amsterdam: 2004. p. 1213-1241.

Büttner-Ennever JA. Patterns of connectivity in the vestibular nuclei. Ann N Y Acad Sci. 1992; 656:363–78. [PubMed: 1599156]

Cannon SC, Robinson DA. Loss of the neural integrator of the oculomotor system from brain stem lesions in monkey. J Neurophysiol. 1987; 57:1383–409. [PubMed: 3585473]

Carleton SC, Carpenter MB. Distribution of primary vestibular fibers in the brainstem and cerebellum of the monkey. Brain Res. 1984; 294:281–98. [PubMed: 6200186]

Chang Y, Yan LH, Zhang FK, Gong KR, Liu MG, Xiao Y, Xie F, Fu H, Chen J. Spatiotemporal characteristics of pain-associated neuronal activities in primary somatosensory cortex induced by peripheral persistent nociception. Neurosci Lett. 2008; 448:134–8. [PubMed: 18805459]

Chen LW, Lai CH, Law HY, Yung KK, Chan YS. Quantitative study of the coexpression of Fos and N-methyl-D aspartate (NMDA) receptor subunits in otolith-related vestibular nuclear neurons of rats. J Comp Neurol. 2003; 460:292–301. [PubMed: 12687692]

Cirelli C, Pompeiano M, D'Ascanio P, Arrighi P, Pompeiano O. c-fos Expression in the rat brain after unilateral labyrinthectomy and its relation to the uncompensated and compensated stages. Neuroscience. 1996; 70:515–46. [PubMed: 8848156]

Curthoys IS, Markham CH, Curthoys EJ. Semicircular duct and ampulla dimensions in cat, guinea pig and man. J Morphol. 1977; 151:17–34. [PubMed: 830956]

D'Ascanio P, Arrighi P, Pompeiano O. Fos-protein expression in noradrenergic locus coeruleus neurons after unilateral labyrinthectomy in the rat. Arch Ital Biol. 1998; 136:83–102. [PubMed: 9492948]

d'Ascanio P, Balaban E, Pompeiano M, Centini C, Pompeiano O. Fos and FRA protein expression in rat precerebellar structures during the Neurolab Space Mission. Brain Res Bull. 2003; 62:203–21. [PubMed: 14698354]

Darlington CL, Lawlor P, Smith PF, Dragunow M. Temporal relationship between the expression of fos, jun and krox-24 in the guinea pig vestibular nuclei during the development of vestibular compensation for unilateral vestibular deafferentation. Brain Res. 1996; 735:173–6. [PubMed: 8905184]

Darlington CL, Smith PF. The recovery of static vestibular function following peripheral vestibular lesions in mammals: the intrinsic mechanism hypothesis. J Vestib Res. 1996; 6:185–201. [PubMed: 8744526]

Duflo SGD, Gestreau C, Tighilet B, Lacour M. Fos expression in the cat brainstem after unilateral vestibular neurectomy. Brain Res. 1999; 824:1–17. [PubMed: 10095037]

Emmers, R.; Akert, K. A stereotaxic atlas of the brain of the squirrel monkey (*Saimiri sciureus*). University of Wisconsin Press; Madison: 1963.

Fukushima K, Kaneko CR. Vestibular integrators in the oculomotor system. Neurosci Res. 1995; 22:249–58. [PubMed: 7478288]

Gacek RR. Location of brain stem neurons projecting to the oculomotor nucleus in the cat. Exp Neurol. 1977; 57:725–49. [PubMed: 923675]

Gerrits, N. Vestibular Nuclear Complex. In: Paxinos, G., editor. The Human Nervous System. Academic Press; Philadelphia: 1990. p. 863-888.

Gerrits NM, Voogd J, Magras IN. Vestibular nuclear efferents to the nucleus raphe pontis, the nucleus reticularis tegmenti pontis and the nuclei pontis in the cat. Neurosci Lett. 1985a; 54:357–62. [PubMed: 3991074]

Gerrits NM, Voogd J, Nas WS. Cerebellar and olivary projections of the external and rostral internal cuneate nuclei in the cat. Exp Brain Res. 1985b; 57:239–55. [PubMed: 3972028]

Goldberg JM, Fernandez C. Physiology of peripheral neurons innervating semicircular canals of the squirrel monkey. I. Resting discharge and response to constant angular accelerations. J Neurophysiol. 1971; 34:635–60. [PubMed: 5000362]

Graybiel AM, Hartwieg EA. Some afferent connections of the oculomotor complex in the cat: an experimental study with tracer techniques. Brain Res. 1974; 81:43–51.

Guo ZL, Moazzami AR, Longhurst JC. Stimulation of cardiac sympathetic afferents activates glutamatergic neurons in the parabrachial nucleus: relation to neurons containing nNOS. Brain Res. 2005; 1053:97–107. [PubMed: 16054113]

Haas CA, Donath C, Kreutzberg GW. Differential expression of immediate early genes after transection of the facial nerve. Neuroscience. 1993; 53:91–9. [PubMed: 7682301]

Hoddevik GH, Dietrichs E, Walberg F. Afferent connections to the abducent nucleus in the cat. Arch Ital Biol. 1991; 129:63–72. [PubMed: 1707258]

Hughes P, Dragunow M. Induction of immediate-early genes and the control of neurotransmitter-regulated gene expression within the nervous system. Pharmacol Rev. 1995; 47:133–78. [PubMed: 7784478]

Jensen DW. Reflex control of acute postural asymmetry and compensatory symmetry after a unilateral vestibular lesion. Neuroscience. 1979; 4:1059–73. [PubMed: 492523]

Jian BJ, Cotter LA, Emanuel BA, Cass SP, Yates BJ. Effects of bilateral vestibular lesions on orthostatic tolerance in awake cats. J Appl Physiol. 1999; 86:552–60.

Kaufman GD, Anderson JH, Beitz AJ. Fos-defined activity in rat brainstem following centripetal acceleration. J Neurosci. 1992; 12:4489–500. [PubMed: 1432106]

Kaufman GD, Anderson JH, Beitz AJ. Otolith-brain stem connectivity: evidence for differential neural activation by vestibular hair cells based on quantification of FOS expression in unilateral labyrinthectomized rats. J Neurophysiol. 1993; 70:117–27. [PubMed: 8395570]

Kaufman GD. Activation of immediate early genes by vestibular stimulation. Ann N Y Acad Sci. 1996; 781:437–442. [PubMed: 8694433]

Kaufman GD, Shinder ME, Perachio AA. Correlation of Fos expression and circling asymmetry during gerbil vestibular compensation. Brain Res. 1999; 817:246–55. [PubMed: 9889379]

Kaufman GD, M. R, Shinder ME. Microarray analysis of vestibular compensation in the gerbil. Neuro Sci. 2003 Abs #703.12.

Kaufman GD. Fos expression in the vestibular brainstem: what one marker can tell us about the network. Brain Res Brain Res Rev. 2005; 50:200–11. [PubMed: 16039721]

Kerman IA, Yates BJ. Regional and functional differences in the distribution of vestibulosympathetic reflexes. Am J Physiol. 1998; 275:R824–35. [PubMed: 9728081]

Kevetter GA, Leonard RB, Newlands SD, Perachio AA. Central distribution of vestibular afferents that innervate the anterior or lateral semicircular canal in the mongolian gerbil. J Vestib Res. 2004; 14:1–15. [PubMed: 15156092]

Killian JE, Baker JF. Electromyographic activity of dorsal neck muscles in squirrel monkeys during rotations in an upright or upside down posture. J Neurophysiol. 2005; 93:2587–99. [PubMed: 15647395]

Kitahara T, Saika T, Takeda N, Kiyama H, Kubo T. Changes in Fos and Jun expression in the rat brainstem in the process of vestibular compensation. Acta Otolaryngol Suppl. 1995; 520(Pt 2): 401–4. [PubMed: 8749173]

Kitahara T, Takeda N, Saika T, Kubo T, Kiyama H. Role of the flocculus in the development of vestibular compensation: immunohistochemical studies with retrograde tracing and flocculectomy using Fos expression as a marker in the rat brainstem. Neuroscience. 1997; 76:571–80. [PubMed: 9015339]

Korte GE. The brainstem projection of the vestibular nerve in the cat. J Comp Neurol. 1979; 184:279–92. [PubMed: 762285]

Korte GE, Mugnaini E. The cerebellar projection of the vestibular nerve in the cat. J Comp Neurol. 1979; 184:265–77. [PubMed: 762284]

Ladpli R, Brodal A. Experimental studies of commissural and reticular formation projections from the vestibular nuclei in the cat. Brain Res. 1968; 8:65–96. [PubMed: 5650812]

Lai CH, Tse YC, Shum DK, Yung KK, Chan YS. Fos expression in otolith-related brainstem neurons of postnatal rats following off-vertical axis rotation. J Comp Neurol. 2004; 470:282–96. [PubMed: 14755517]

Lazarov NE. Comparative analysis of the chemical neuroanatomy of the mammalian trigeminal ganglion and mesencephalic trigeminal nucleus. Prog Neurobiol. 2002; 66:19–59. [PubMed: 11897404]

Lois JH, Rice CD, Yates BJ. Neural circuits controlling diaphragm function in the cat revealed by transneuronal tracing. J Appl Physiol. 2009; 106:138–52. [PubMed: 18974365]

Marshburn TH, Kaufman GD, Purcell IM, Perachio AA. Saccule contribution to immediate early gene induction in the gerbil brainstem with posterior canal galvanic or hypergravity stimulation. Brain Res. 1997; 761:51–8. [PubMed: 9247065]

McCrea RA, Baker R, Delgado-Garcia J. Afferent and efferent organization of the prepositus hypoglossi nucleus. Prog Brain Res. 1979; 50:653–65. [PubMed: 551460]

McCrea RA, Baker R. Anatomical connections of the nucleus prepositus of the cat. J Comp Neurol. 1985; 237:377–407. [PubMed: 2995460]

Melia KR, Ryabinin AE, Schroeder R, Bloom FE, Wilson MC. Induction and habituation of immediate early gene expression in rat brain by acute and repeated restraint stress. J Neurosci. 1994; 14:5929–38. [PubMed: 7931554]

Moran LB, Graeber MB. The facial nerve axotomy model. Brain Res Brain Res Rev. 2004; 44:154–78. [PubMed: 15003391]

Morgan JI, Curran T. Stimulus-transcription coupling in the nervous system: involvement of the inducible proto-oncogenes fos and jun. Annu Rev Neurosci. 1991; 14:421–51. [PubMed: 1903243]

Muigg P, Scheiber S, Salchner P, Bunck M, Landgraf R, Singewald N. Differential stress-induced neuronal activation patterns in mouse lines selectively bred for high, normal or low anxiety. PLoS One. 2009; 4:e5346. [PubMed: 19399175]

Nestler EJ. Review. Transcriptional mechanisms of addiction: role of DeltaFosB. Philos Trans R Soc Lond B Biol Sci. 2008; 363:3245–55. [PubMed: 18640924]

O'Hara BF, Young KA, Watson FL, Heller HC, Kilduff TS. Immediate early gene expression in brain during sleep deprivation: preliminary observations. Sleep. 1993; 16:1–7. [PubMed: 8456228]

Panneton WM, McCulloch PF, Sun W. Trigemino-autonomic connections in the muskrat: the neural substrate for the diving response. Brain Res. 2000; 874:48–65. [PubMed: 10936223]

Pettorossi VE, Grassi S, Errico P, Barmack NH. Role of cerebellar nodulus and uvula on the vestibular quick phase spatial constancy. Acta Otolaryngol Suppl. 2001; 545:155–9. [PubMed: 11677731]

Raphan T, Matsuo V, Cohen B. Velocity storage in the vestibulo-ocular reflex arc (VOR). Exp Brain Res. 1979; 35:229–48. [PubMed: 108122]

Raphan T, Cohen B. Organizational principles of velocity storage in three dimensions. The effect of gravity on cross-coupling of optokinetic after-nystagmus. Ann N Y Acad Sci. 1988; 545:74–92. [PubMed: 3239884]

Raphan T, Schnabolk C. Modeling slow phase velocity generation during off-vertical axis rotation. Ann N Y Acad Sci. 1988; 545:29–50. [PubMed: 3149166]

Sato Y, Kawasaki T, Ikarashi K. Afferent projections from the brainstem to the three floccular zones in cats. II. Mossy fiber projections. Brain Res. 1983; 272:37–48. [PubMed: 6616198]

Sato Y, Kanda K, Ikarashi K, Kawasaki T. Differential mossy fiber projections to the dorsal and ventral uvula in the cat. J Comp Neurol. 1989; 279:149–64. [PubMed: 2913059]

Saxon DW, Anderson JH, Beitz AJ. Transtympanic tetrodotoxin alters the VOR and Fos labeling in the vestibular complex. Neuroreport. 2001; 12:3051–5. [PubMed: 11568635]

Saxon DW. Distribution of Fos labeling in the inferior olive following transient blockade of the VIIIth cranial nerve. Brain Res. 2003; 966:134–49. [PubMed: 12646317]

Sekerkova G, Ilijic E, Mugnaini E, Baker JF. Otolith organ or semicircular canal stimulation induces c-fos expression in unipolar brush cells and granule cells of cat and squirrel monkey. Exp Brain Res. 2005; 164:286–300. [PubMed: 15940501]

Shaw MD, Baker R. Direct projections from vestibular nuclei to facial nucleus in cats. J Neurophysiol. 1983; 50:1265–80. [PubMed: 6319618]

Shinder ME, Perachio AA, Kaufman GD. VOR and Fos response during acute vestibular compensation in the Mongolian gerbil in darkness and in light. Brain Res. 2005a; 1038:183–97. [PubMed: 15757634]

Shinder ME, Perachio AA, Kaufman GD. Fos responses to short-term adaptation of the horizontal vestibuloocular reflex before and after vestibular compensation in the Mongolian gerbil. Brain Res. 2005b; 1050:79–93. [PubMed: 15978560]

Shinder ME, Ramanathan M Jr. Kaufman GD. Asymmetric gene expression in the brain during acute compensation to unilateral vestibular labyrinthectomy in the Mongolian gerbil. J Vestib Res. 2006; 16:147–69. [PubMed: 17538204]

Snyder JS, Radik R, Wojtowicz JM, Cameron HA. Anatomical gradients of adult neurogenesis and activity: young neurons in the ventral dentate gyrus are activated by water maze training. Hippocampus. 2009; 19:360–70. [PubMed: 19004012]

Somana R, Walberg F. A re-examination of the cerebellar projections from the gracile, main and external cuneate nuclei in the cat. Brain Res. 1980; 186:33–42. [PubMed: 7357449]

Spencer RF, Wenthold RJ, Baker R. Evidence for glycine as an inhibitory neurotransmitter of vestibular, reticular, and prepositus hypoglossi neurons that project to the cat abducens nucleus. J Neurosci. 1989; 9:2718–36. [PubMed: 2570136]

Sylvestre PA, Choi JT, Cullen KE. Discharge dynamics of oculomotor neural integrator neurons during conjugate and disjunctive saccades and fixation. J Neurophysiol. 2003; 90:739–54. [PubMed: 12672779]

Tan H, Gerrits NM. Laterality in the vestibulo-cerebellar mossy fiber projection to flocculus and caudal vermis in the rabbit: a retrograde fluorescent double-labeling study. Neuroscience. 1992; 47:909–19. [PubMed: 1374542]

Vibert N, Bantikyan A, Babalian A, Serafin M, Muhlethaler M, Vidal PP. Post-lesional plasticity in the central nervous system of the guinea-pig: a "top-down" adaptation process? Neuroscience. 1999; 94:1–5. [PubMed: 10613489]

Yates BJ, Holmes MJ, Jian BJ. Adaptive plasticity in vestibular influences on cardiovascular control. Brain Res Bull. 2000; 53:3–9. [PubMed: 11033202]
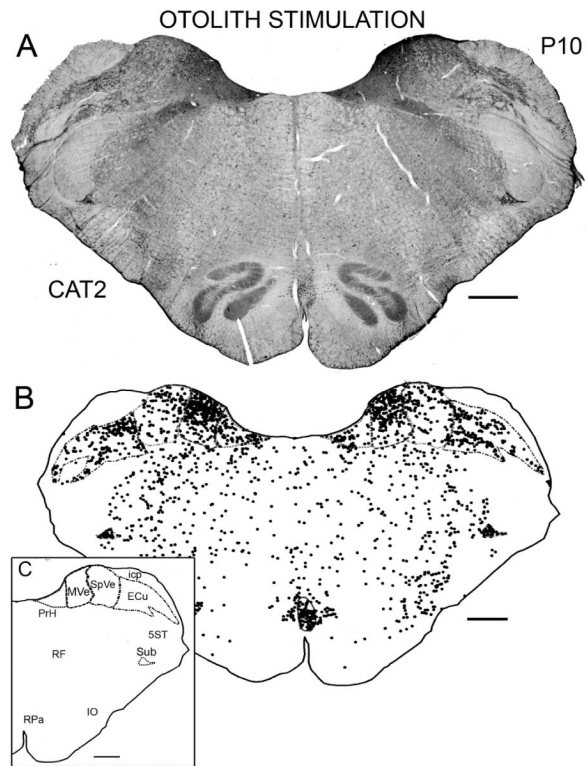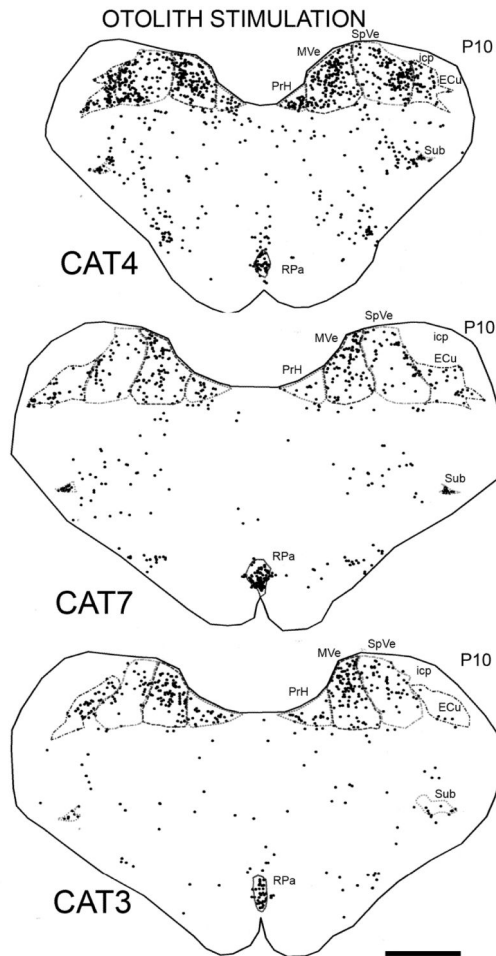
Figure 1.
A. Photomontage of a section at about P10 from CAT2; this animal was subjected to otolith stimulation. Scale bar 1 mm. **B.** Plot of labeled cells on the section shown in **A. C.** The inset identifies the structures that are outlined in **B**. Each dot represents one labeled cell. The Bregma level is indicated in the upper right. Scale bars 1 mm. Abbreviation icp, inferior cerebellar peduncle.
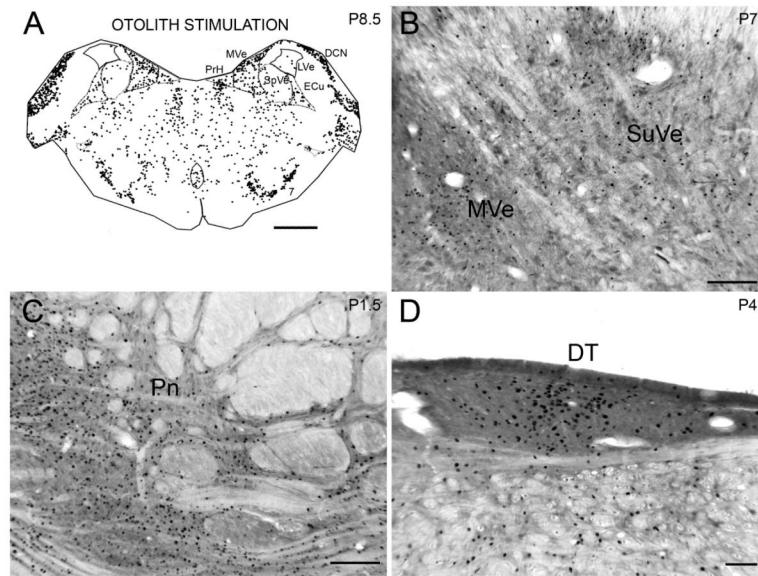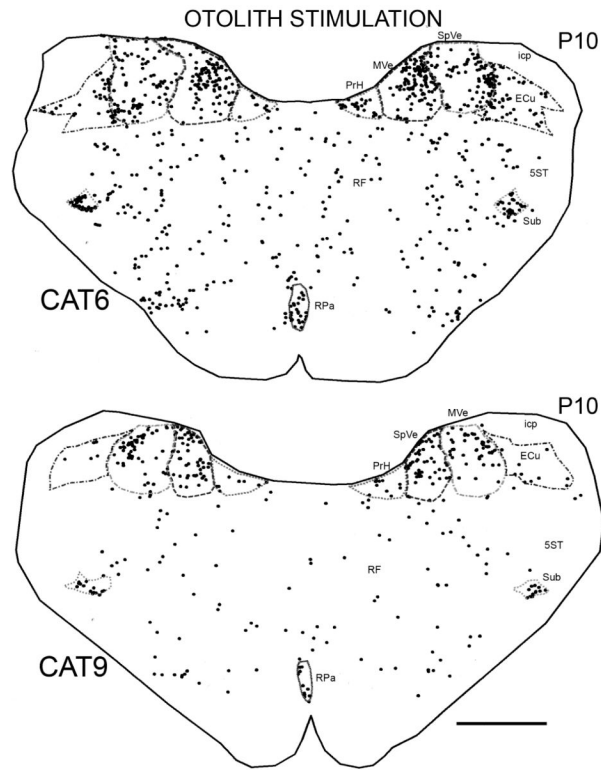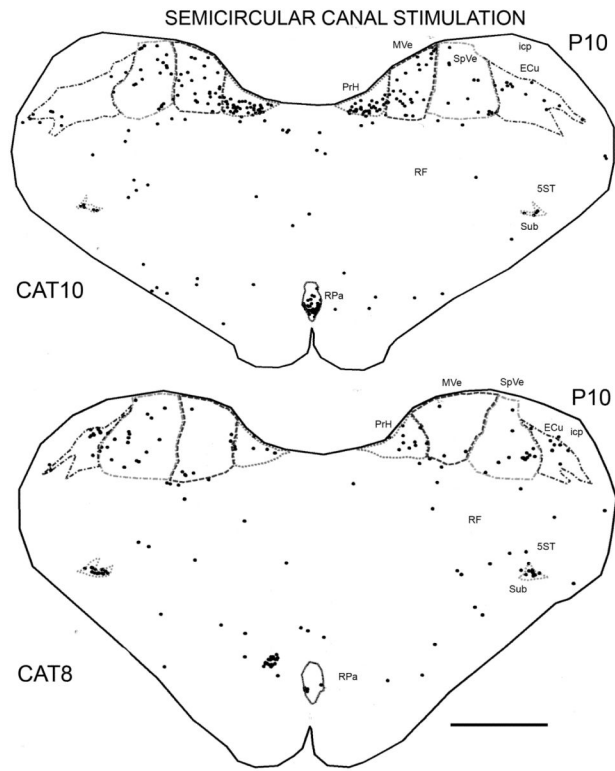
Figure 2.
A. Distribution of cells with labeled nuclei on a section at about P8.5 from CAT2, the same case illustrated in Fig.1. Note the paucity of labeled cells in the LVe. Scale bar 2 mm. **B.** Labeled cells in the SuVe on a section from CAT2 on a section at about P7.0. Scale bar 500 μm. **C.** Labeled cells in the dorsal tegmental nucleus, (DT), CAT2, on a section at about P4.1. **D**. Labeled cells in the pontine gray, Pn, of CAT2, section at about P0.1. Scale bar (C, D) 500 μm.

Figure 3.
Plots showing the distribution of labeled cells on sections at about P10.0 in CAT4, CAT7 and CAT3 (otolith stimulation). Conventions as in Fig. 1A. Scale bar 2 mm.
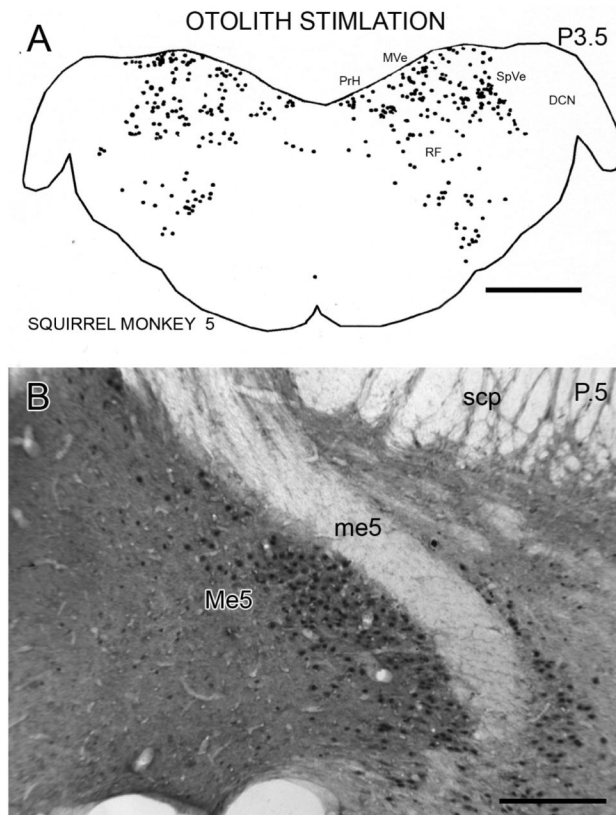
Figure 4.
Plot showing the distributions of labeled cells on sections at about P10.0 in CAT6 and CAT9 (otolith stimulation). Scale bar 2 mm.

Figure 5.
Plots showing the distributions of labeled cells on sections at about P10.0 in CAT8 and CAT10 (semicircular canal stimulation). Scale bar 2 mm.

Figure 6.
A. Plot of the distribution of Fos-labeled cells in a section from squirrel monkey SM5, at about P3.5. Conventions as in Fig. 1A. Scale bar 2 mm. **B.** Photomicrograph of Fos-immunoreactivity in the nucleus of the mesencephalic tract of the trigeminal (Me5) on a section at about P0.5. Scale bar 500 μm. Abbreviations DCN, dorsal cochlear nucleus, me5, mesencephalic tract of the trigeminal, scp, superior cerebellar peduncle.

Table 1

Number of Fos-ir cells in different structures in the cat brainstem as illustrated in Figures 1 and 3-5. The numbers are the total from both sides

Case	MVe	SpVe	PrH	ECu	Sub	RPa
CAT2	454	212	119	368	71	81
CAT4	295	284	48	109	20	38
CAT7	150	88	28	61	30	84
CAT3	173	75	46	38	13	31
CAT6	206	167	33	79	62	24
CAT9	97	105	17	15	26	11
CAT8	10	32	14	17	21	6
CAT10	52	33	67	18	8	41